

A Novel Scanning Lens Instrument For Evaluating Fresnel Lens Performance: Equipment Development And Initial Results

Rebeca Herrero , David C. Miller , Sarah R. Kurtz , Ignacio Antón
and Gabriel Sala

Abstract: A system dedicated to the optical transmittance characterization of Fresnel lenses has been developed at NREL, in collaboration with the UPM. The system quantifies the optical efficiency of the lens by generating a performance map. The shape of the focused spot may also be analyzed to understand change in the lens performance. The primary instrument components (lasers and CCD detector) have been characterized to confirm their capability for performing optical transmittance measurements. Measurements performed on SoG and PMMA lenses subject to a variety of indoor conditions (*e.g.*, UV and damp heat) identified differences in the optical efficiency of the evaluated lenses, demonstrating the ability of the Scanning Lens Instrument (SLI) to distinguish between the aged lenses.

Keywords: Solar concentrators, characterization, CCD, reliability, durability

INTRODUCTION

The optical performance of a photovoltaic concentrator is dependent on the efficiency of its transmittance, which may be defined as the ratio of the flux collected out of the concentrator, P_{out} (W), to the flux arriving at the aperture of the concentrator, P_{in} (W). Integrating the transmittance function over the angular, spatial and spectral bounds of the incident radiation leads to the most common figure of merit for concentrator optics characterization: the optical efficiency η .

Two key components must be identified to perform suitable optical efficiency measurements: the illumination source and the flux detector. Because the optical efficiency depends on the angular, spatial and spectral features of the incident light, it therefore has to be representative of the designated light source for PV concentrators: the standard solar disc. The optical efficiency also depends on the detector, including its optical coupling with the concentrator, its spectral response, and its physical size.

Many concentrating photovoltaic (CPV) systems use a Fresnel lens as the primary optical element (POE) to concentrate sunlight onto a photovoltaic receiver. To measure the absolute lens efficiency, it is necessary to use a sizeable white light source. However, to study local lens defects or material aging (that can be wavelength-dependent), it is desirable to measure with monochromatic light across the lens [1].

Scanning the concentrator with a small-diameter laser can also be advantageous to assess the type and morphology of lens defects.

A system dedicated to the optical transmittance characterization of aged Fresnel lenses has been developed at NREL, in collaboration with the IES-UPM. The primary instrument components (lasers and a CCD detector) of the so-called "Scanning Lens Instrument" (SLI) have been characterized to quantify its measurement capability. Initial measurements were obtained for different lens samples, made from either solar grade polymethyl methacrylate (PMMA) or silicone-on-glass (SoG), subject to a variety of indoor aging conditions. The wavelength-specific optical efficiency values of the aged lenses have been compared relative to their spectral transmittance and absolute optical efficiency (verified at IES-UPM by the CPV solar simulator Helios 3198 [2]) in order to better understand the SLI capabilities

SLI: CHARACTERIZATION AND MEASUREMENTS

The SLI is intended to quantify the effect of local defects as well as performance changes that result from lens degradation. The SLI shown in Figure 1 includes: a lens fixture (to secure the lens specimen in place), a set of small-diameter lasers (wavelengths of 405 nm, 532 nm, or 650 nm, with nominal beam diameters given by the manufacture of 1.3 mm, 1 mm,

and 1.6 mm, respectively) that illuminate the lens by scanning its aperture area using an x-y- motor stage, and a charge-coupled device (CCD) camera at the focal point of the lens, to measure the focused light.

The quantitative analysis of the CCD signal across the lens aperture is performed with respect to an initial baseline measurement of the laser without the lens present. Therefore, the optical efficiency is defined as the ratio of the laser light focused by the lens relative to the intensity of the laser source. A performance map quantifying the optical efficiency may be generated for the lens using the x-y-motor stage, and from this map an average value of optical efficiency can be determined for the lens. Neutral density filters are used to attenuate the laser signal to avoid saturating the CCD detector. The shape of the focused spot may also be analyzed to understand changes in the lens performance.

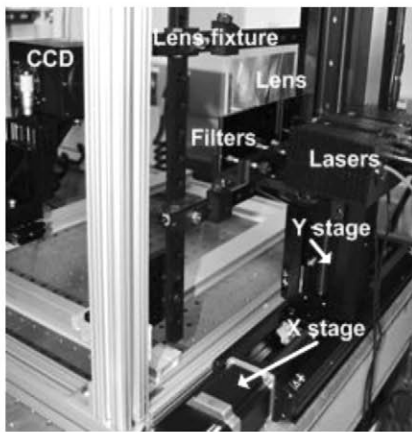


FIGURE 1. Image of the instrument components.

In the SLI, the light focused by the Fresnel lens is measured by a Si CCD camera. Both the quantum efficiency (QE) and the angular response (AR) of the detector were verified in order to exclude spurious effects the CCD detector could have on lens measurements. The laser properties (*i.e.*, spatial and angular size) create differences in the results for each of the lasers. The spots from the three lasers, together with their angular distributions, have been inspected with the CCD camera mounted in front of each laser [3]. In the CCD image, concentric circumferences about the center of the measured light distribution can be traced to obtain the average value of intensity related to the pixels that form each circumferencing arc. The angular distribution profiles for the average intensity values are plotted versus the radius at the circumference in Figure 2. In the figure, all three SLI lasers are narrower in angular size than the AM1.5 solar disc within which 90% of the energy is contained.

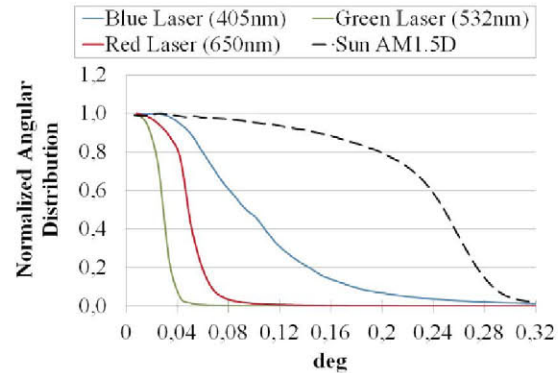


FIGURE 2. Normalized angular distribution of lasers measured by a CCD camera when focusing to infinity. The lasers are compared with the sun's angular distribution

The laser can be partially coherent, meaning interference and speckle noise can affect SLI measurements [4]. If this coherence is significant enough to modify the measurements, a refractive random surface diffuser could be added to generate multiple light sources, reducing the speckle noise.

Due to the fact that the lasers have different angular and spatial distributions, the properties of the light focused by the lens depended not only on the evaluated optics but also on the laser used in the measurement. The light spots focused by a representative PMMA lens are presented in Figure 3.

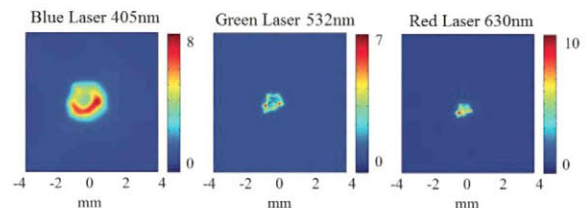


FIGURE 3. Light focused by a PMMA lens measured by the CCD detector for the three lasers of the SLI instrument

If there is not a defined photovoltaic receiver area for the Fresnel lens under characterization, a detector size has to be assumed to calculate the optical efficiency. The size of the focused region is complicated by the influence of the noise background. Some precautions have to be taken using noise background image subtraction for the cooled CCD detector (with a large dynamic range and a high bit depth, able to record high and low values together), so that the low intensity measurement signal is not buried in the noise.

The SLI was confirmed to be able to identify micro-scale lens defects, such as scratched lens facets. For example, we observed that a minor scratch in the silicon facets of a SoG lens can produce a decrease of ~ 1% efficiency (Figure 4). The green laser (1 mm in diameter) was chosen to identify this kind of small

defects due to its smallest size. In Figure 4, the scan resolution (distance between laser positions in consecutive measurements) is 0.2 mm, and the laser diameter is 1 mm. The pixel resolution is around 0.0074 mm.

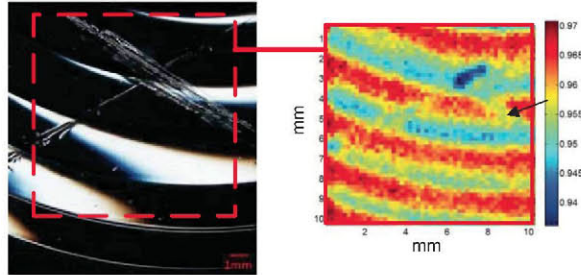


FIGURE 4. Lens measurement at scratch sites: (left) optical image of a lens (separately scratched on its front and back), (right) optical efficiency map at the scratched region.

The size of the laser is larger than the facets of the lens. The scan resolution is adequate (here, depending mainly on the size of the scratch) to replicate the shape of the defect in the measured optical efficiency map. A detailed image of the scratch resolved in the measurement is presented in Figure 5, in which it can be observed that the size of the scratch is very close to the one that is measured by the SLI with a scan resolution of 2 mm (*i.e.*, distance between laser positions in consecutive measurements).

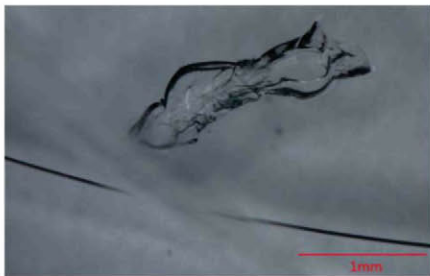


FIGURE 5. Detailed image of the scratch in the silicone facet.

Separate PMMA and SoG lenses were subjected to indoor aging conditions of: 65°C/85%RH (1000 hours), 85°C/85%RH (1000 h), 60°C/60%RH/2.5x UV (1000 h in an Atlas Ci4000 Xe-arc Weather-ometer), or 1.5x UV “Suntest” (temperature and humidity uncontrolled in an Atlas Xe-arc Suntest CPS). The lenses were then characterized on the central 1-cm² region using a Perkin-Elmer Lambda 900 spectrophotometer, allowing for subsequent calculation of solar-weighted transmittance and yellowness index. To evaluate the instrument capabilities, these lenses were also measured on the

SLI at NREL and the CPV solar simulator at IES-UPM.

CPV HELIOS 3198 SOLAR SIMULATOR

The solar simulator Helios 3198 developed by the IES-UPM uses a Xenon flash lamp and a 2-meter-diameter collimator mirror that reproduces at the input aperture of the lens a light distribution similar to the Sun, not only in angular size $L_{in}(\varphi, \theta)$ but also the equivalent AM1.5D spectrum $S_{in}(\lambda)$ [2].

The efficiency in the solar simulator is calculated as the ratio of power at the input and output of the Helios concentrator, Equation 1. The irradiance G_{in} at the entrance of the lens area (A_{lens}) is measured by component reference cells, and the irradiance G_{out} at the focus of the lens is measured by a typical III-V 3-junction (3J) solar cell (GaInP/GaInAs/Ge) of area (A_{MJ}) 1cm².

$$\eta(S_{in}(\lambda), L_{in}(\varphi, \theta)) = \frac{G_{out} \cdot A_{MJ}}{G_{in} \cdot A_{lens}} \quad (1)$$

The multi-junction solar cell used as a flux detector was characterized in a CPV solar cell tester to evaluate its electrical characteristics under concentration and different spectral conditions. The spectral response of the multi-junction solar cell was also studied to confirm its similarity with that of the component reference cells. The light spot size for each lens is also measured using a CCD camera (with long/short pass filters), in order to confirm that the multi-junction cell is large enough to measure the complete area of light concentrated by the Fresnel lens [5].

The Xenon-filled gas discharge lamp of the Helios simulator operates in a ‘pulse’ optical mode, achieving high radiances with spectrum variations during the pulse decay. The optical efficiency of the Fresnel lens can be plotted versus the ratio of DNI given by top and middle component reference cells calibrated under AM1.5D spectrum (*i.e.*, spectral matching ratio SMR) of the incoming light as shown in Figure 6 and Figure 7. Comparing these figures, it can be seen that the PMMA lens aged with 1.5x UV needs to be illuminated with a more blue-rich spectrum than the reference lens, to have the same current limited condition in the middle subcell (*i.e.*, the middle cell is limiting when the red line value is kept constant). The 1.5x UV aged specimen was uniquely visually discolored (yellow) after aging, with a measured decrease in transmittance from 350-550 nm (Figure 8).

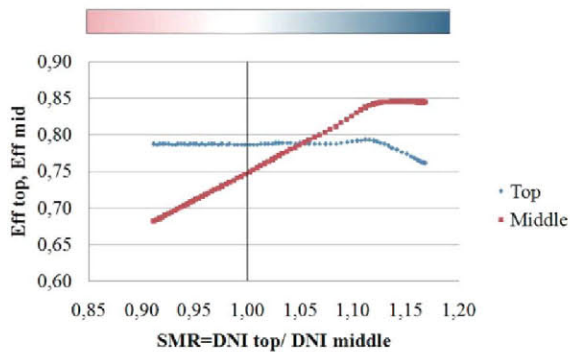


FIGURE 6. Optical efficiencies for PMMA reference lens versus spectral matching ratio measured using the Helios CPV solar simulator.

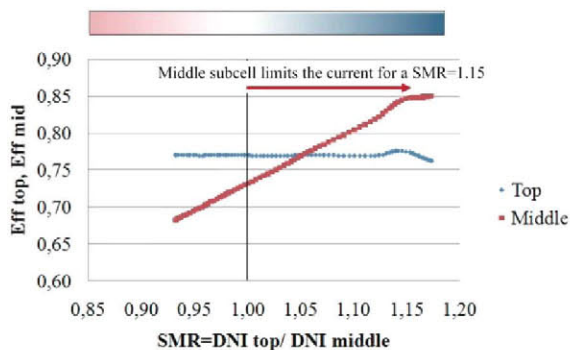


FIGURE 7. Optical efficiencies for PMMA lens after 1.5x UV aging versus spectral matching ratio, measured using the Helios CPV solar simulator.

RESULTS

These results are intended to provide examples of the SLI's capability to identify defects and the aging of lenses. The results here do not constitute a formal lens degradation study.

The SLI does not calculate an absolute value of efficiency because the measurement is performed with monochromatic light with different angular sizes. Therefore, its results are normalized to study the relative deviations between the aged lenses.

For SLI, the optical efficiency of the lens is presented for the three lasers (*i.e.*, blue 405 nm, green 532 nm, and red 650 nm). For the CPV solar simulator, the optical efficiency is given for top and middle subcells (*i.e.*, red- and blue-rich spectrums, respectively). All the wavelengths measured using the SLI are effectively integrated in the top subcell for the solar simulator. Thus, laser and subcell optical efficiency values can only be compared generally, because the top cell response for the Helios simulator (that integrates the three laser wavelengths) is related

to a particular angular size of the light, whereas the CCD measurement for the SLI is related to the angular size of the laser used.

For the PMMA lenses, three different aged samples are compared: Reference ("REF") lens (unaged), 85C/85%RH and Suntest. The hemispherical transmittances of PMMA lenses are presented in Figure 8, for the lenses, placed against the 1 cm x 1.5 cm aperture of the integrating sphere.

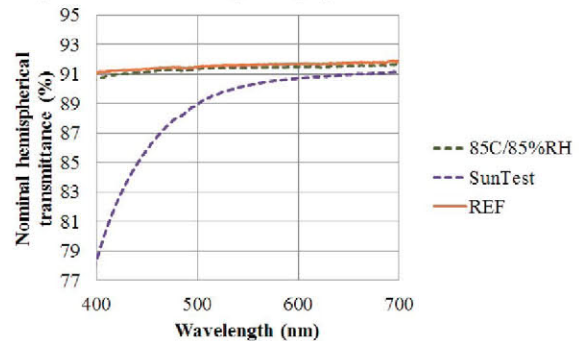


FIGURE 8. Hemispherical transmittance (spectrometer) measurements for some PMMA lenses.

From both SLI (in Figure 9) and the Helios simulator (in Figure 10), the higher optical efficiency for short wavelengths occurs for the reference lens, with the lowest efficiency for the Suntest lens. From the SLI, the shortest wavelength (blue laser) corresponds to the lowest optical efficiency in the aged lenses. Wavelength-specific results cannot be revealed by the Helios simulator, because all wavelengths are combined in the top subcell efficiency. The reduced performance for the Suntest-aged PMMA lens in Figure 9 and Figure 10 is attributed to an absorbing chromophore species evident in the measured transmittance spectra (Figure 8). Curiously discoloration was not observed for the 85°C/85%RH and 60°C/60%RH/2.5x UV aged specimens, suggesting that UV (without moisture) is critical to discoloration. Unlike the PMMA lens aged at 65°C/85%RH, the PMMA lens aged at 85°C/85%RH was changed in shape (presumably gravity sag for the specimen held horizontally [aperture facing the chamber top] during aging). Shape change for the 85°C/85%RH lens also occurs at the micro-scale (shape change of the chromatic sensitive facets). The intensity between lasers shows the same tendency, but not the same relative variation between lenses (*i.e.*, transmittance measurements identify a 14% loss for 405 nm for the SunTest lens with no notable loss for the 85°C/85%RH lens, while the SLI identifies a 16% loss for the Suntest lens compared with a 12% loss for the 85°C/85%RH lens). One key difference between the measurements is that the spectrophotometer uses an integrating sphere (including the diffuse

transmittance), whereas the SLI can only detect the direct transmittance

In the Figure 9 and Figure 12 the scan resolution (distance between laser positions in consecutive measurements) is 1 mm.

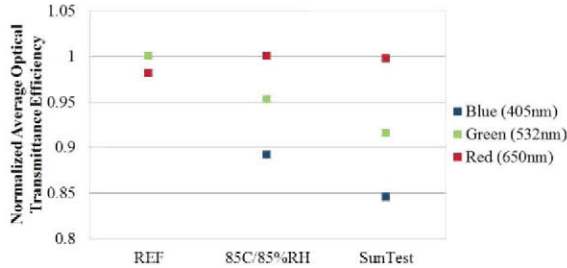


FIGURE 9. Optical efficiency of PMMA lenses measured using the SLI.

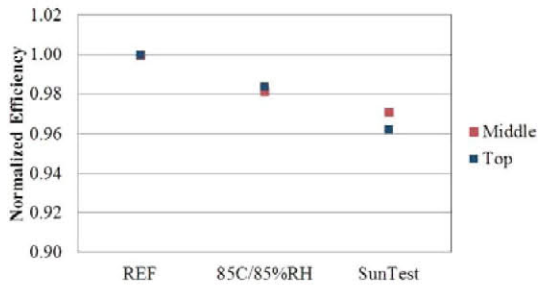


FIGURE 10. Optical efficiency of PMMA lenses measured using the Helios CPV solar simulator.

For the SoG lenses, two different aged samples are compared in Figure 12: the unaged lens, referred to as reference (REF), and 85C/85%RH aged lenses.

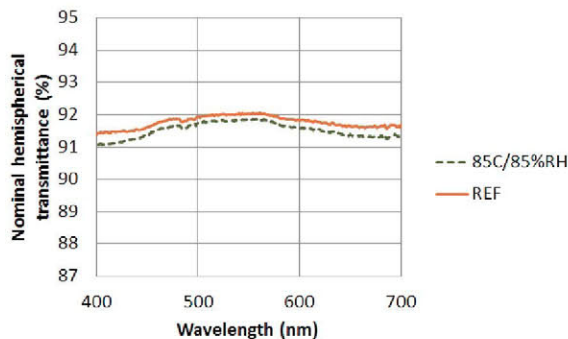


FIGURE 11. Hemispherical transmittance (spectrometer) measurements for some SoG lenses.

From both the SLI measurements in Figure 12 and the Helios simulator measurements in Figure 13, the higher optical efficiency for short wavelengths occurs for the SoG reference lens.

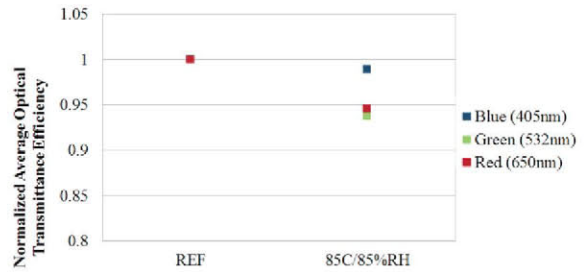


FIGURE 12. Optical efficiency of SoG lenses measured using the SLI .

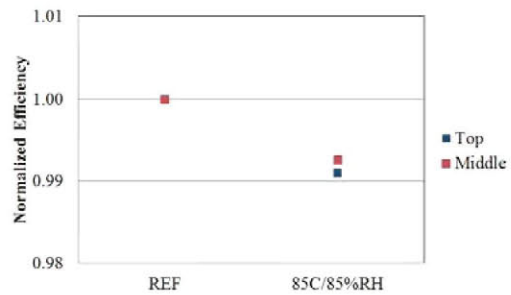


FIGURE 13. Optical efficiency of SoG lenses measured using the Helios CPV solar simulator

One possible explanation for the decrease in optical efficiency for the 85C/85%RH aged SoG lens is glass corrosion. Glass corrosion would not necessarily show up for a spectrophotometer with an integrating-sphere, like we used in Figure 11. The surface features observed in a microscope for the 85C/85%RH aged lens are also consistent with glass corrosion.

TABLE 1. Summary of the causes and consequences of degradation in Fresnel lenses investigated by the SLI and the solar simulator

Kind of degradation	Material	Effect on concentrator	How to identify
85C/85%RH	PMMA	Δ shape \rightarrow Δ focus	SLI or Helios simulator
Suntest	PMMA	Discoloration \rightarrow optical absorption	Spectrophotometer, SLI or Helios
85C/85%RH	SoG	Glass corrosion \rightarrow optical scattering	AFM techniques

CONCLUSIONS

The “Scanning Lens Instrument” (SLI) has been constructed for CPV lens characterization. Key results include:

The SLI instrument covers the compulsory requirement of collimation for CPV characterization by using a feasible and affordable implementation. The SLI equipment does not identify an absolute optical efficiency value, but the effects of poor optical design, imperfections on lens fabrication, and lens aging can be quantified and diagnosed.

Component characterization and image processing have been performed to validate the SLI results. Background noise correction of the measurement is a limiting source of error.

Both PMMA and SoG lenses have been measured in the SLI and Helios CPV solar simulator. The results, compared to spectrophotometer (transmittance) measurements, identify the formation of chromophore species for UV/temperature aged PMMA, shape change of the lens or PMMA aged in damp heat, and corrosion of the glass superstrate for SoG lens aged in damp heat.

ACKNOWLEDGMENTS

This work has been partially supported by the Spanish Ministry of Economy and Competitiveness under Project SIGMA-E (IPT-2011-1218-92000).

Rebeca Herrero is thankful to the Spanish Ministerio de Educación for her FPU grant, and to the UPM for her grant from Consejo Social. This work was supported by the U.S. Department of Energy under Contract No. DE-AC36-08GO28308 with the National Renewable Energy Laboratory.

REFERENCES

- 1 D. C. Miller and S. R. Kurtz, “Durability of Fresnel lenses: A review specific to the concentrating photovoltaic application,” *Solar Energy Materials and Solar Cells*, vol. 95, no. 8, pp. 2037–2068, Agosto 2011.
- 2 C. Domínguez, I. Antón, and G. Sala, “Solar simulator for concentrator photovoltaic systems,” *Optics Express*, vol. 16, no. 19, pp. 14894–14901, 2008.
- 3 R. Herrero, I. Antón, M. Vivar, and G. Sala, “Characterization of concentrator optical surfaces based on CCD camera measurement,” in *24th European Photovoltaic Solar Energy Conference*, 2009.
- 4 Hornung, T., “Analytical investigation of diffraction in Fresnel lens concentrators,” in *7th International Conference on Concentrating Photovoltaic Systems 2011*, 2012, pp. 93–96.
- 5 R. Herrero, M. Victoria, C. Domínguez, S. Askins, I. Antón, and G. Sala, “Concentration photovoltaic optical system irradiance distribution measurements and its effect on multijunction solar cells,” *Progress in Photovoltaics: Research and Application*, 2011.